Molecular Dynamics Study of the Liquid−Vapor Interface of Acetonitrile: Equilibrium and Dynamical Properties

Sandip Paul and Amalendu Chandra

Department of Chemistry, Indian Institute of Technology, Kanpur, India 208016

Received: September 7, 2005

The equilibrium and dynamical properties of the liquid−vapor interface of pure acetonitrile are studied by means of molecular dynamics simulations. Both nonpolarizable and polarizable models are employed in the present study. For the nonpolarizable model, the simulations are carried out for two different system sizes and at two different temperatures whereas the simulation with the polarizable model is done for a single system. The inhomogeneous density, anisotropic orientational profile, the width of the interface, and also the surface tension are calculated at room temperature and also at a lower temperature of 273 K. The dynamical aspects of the interface are investigated in terms of the single-particle dynamical properties such as the relaxation of velocity autocorrelation and the translational diffusion coefficients along the perpendicular and parallel directions and the dipole orientational relaxation of the interfacial acetonitrile molecules. The results of the interfacial dynamics are compared with those of the corresponding bulk phases at both temperatures. The convergence of the calculated results with respect to the length of simulation runs and the system size are also discussed.

1. Introduction

This paper is concerned with the equilibrium and dynamical behavior of acetonitrile liquid−vapor interface under normal and cold conditions. A detailed knowledge of the molecular properties of liquid−vapor interfaces of molecular liquids is important in the understanding of equilibrium and dynamical aspects of various chemical processes that occur at such interfaces. The molecular environment of a liquid−vapor interface is highly inhomogeneous and anisotropic, and thus the solvent effects on a chemical process occurring at an interface can be quite different from that in a bulk liquid where the molecular environment is homogeneous and isotropic on average. This fact has already been demonstrated both experimentally and theoretically for a number of interfacial chemical processes.[1,2]

Recent experimental studies of the molecular behavior of liquid−vapor interfaces primarily involve the surface-specific nonlinear spectroscopic methods such as second harmonic[1] and sum frequency generation[3] techniques. These methods have been used to investigate a wide variety of interfaces involving pure water or aqueous solutions containing another solvent or a solute species.[1,3−15] Other experimental methods such as neutron reflectivity, X-ray diffraction, and mass spectroscopic measurements have also been used in recent years for studying the molecular nature of liquid−vapor interfaces.[16−19] Eisenthal and co-workers[14] investigated the orientational structure of acetonitrile molecules at the liquid−vapor interface of water−acetonitrile mixtures of varying composition by using the method of second harmonic generation. For higher acetonitrile concentration of the mixtures, the interfacial acetonitrile molecules were found to orient parallel to the surface. Very recently, Somorjai and co-workers[15] used the method of sum frequency generation to investigate the orientational structure of pure acetonitrile and also of acetonitrile dissolved in water and carbon tetrachloride. The tilt angle of the molecular axis of acetonitrile molecules with respect to surface normal was found to be higher in pure acetonitrile than that in acetonitrile−water mixtures. However, differences exist between the results of these two studies (refs 14 and 15) with respect to the magnitude of tilting angle and degree of orientational order of acetonitrile molecules at liquid−vapor interfaces.

Theoretical studies of liquid−vapor interfaces have primarily involved the methods of computer simulations,[2,20−34] although other analytical techniques such as the lattice-gas model, integral equation, and density functional theories have also been employed.[35−38] In the context of the present study, we note the work of Mountain,[31] who investigated the inhomogeneous density and orientational structure of thin films of pure water, acetonitrile, and water−acetonitrile mixtures by means of molecular dynamics simulations. For the surface of pure acetonitrile, the molecules were found to orient more parallel to the surface although no quantitative analysis of the tilting angle of interfacial molecules was presented. Also, other equilibrium quantities of the interfaces such as the interfacial width and surface tension were not calculated in this simulation study. This could partly be due to the relatively smaller system size that was employed in this study so that the results correspond more to the behavior of molecular thin films rather than a liquid−vapor interface. A larger system size has been considered in a very recent study[34] of the structural and dynamical properties of liquid−vapor interfaces of water-acetonitrile mixtures. This latter study has employed nonpolarizable models of both water and acetonitrile and the calculations have been done at room temperature only. Thus, the polarizability and temperature effects on interfacial properties of acetonitrile have not been addressed yet. We note that acetonitrile is an important molecular solvent. Unlike water, acetonitrile molecules have both hydrophobic (methyl) and hydrophilic (cyanide) groups and their structural and dynamical properties in the bulk liquid phase have been thoroughly examined in recent years.[39−42] Clearly, there is a need to make a detailed study of the molecular behavior of acetonitrile at

10.1021/jp055047r CCC: $30.25
Published on Web 10/12/2005

liquid−vapor interfaces where the properties can be substantially different from those of the bulk phases. Also, the difference between the bulk and interfacial properties can significantly depend on temperature. In fact, the diffusive modes of the bulk acetonitrile have already been shown to be rather sensitive to the variation of temperature.[39]

In the present work, we have carried out molecular dynamics simulations of liquid−vapor interface of acetonitrile using both nonpolarizable and polarizable models. For the nonpolarizable model, the simulations are carried out at two different temperatures of 298 and 273 K whereas the simulation with the polarizable model is done at 298 K only because of the high computational cost that is involved in dealing with the polarization calculations. Also, for the nonpolarizable model, the simulations are performed for two different system sizes (864 and 1372 molecules) at 298 K to verify the convergence of the calculated results with respect to the size of the simulation systems.

We have calculated various equilibrium properties of the interface such as density and orientational profiles, the interfacial width, and the surface tension. We have also explored the dynamical aspects of the interface by computing the relaxation of the perpendicular and parallel components of the velocity autocorrelation function and diffusion and also the relaxation of single-particle dipole orientational correlation function of interfacial acetonitrile molecules. The dynamical properties of the interface are compared with those of the bulk phase. The effects of changing temperature are also investigated by comparing the results of various equilibrium and dynamical properties that are obtained at the two different temperatures considered in this study: 298 and 273 K. The variation of the dipole moment of acetonitrile molecules across the liquid−vapor interface is also investigated at 298 K by employing a polarizable model of acetonitrile.

The organization of the rest of the paper is as follows. In section 2, we describe the details of the nonpolarizable model for acetonitrile and the simulation method including the construction of the interfaces. The results of the structure of interfaces and surface tension as produced by the nonpolarizable model are presented in section 3. In section 4, we discuss the dynamical properties of the interface for the nonpolarizable model. In section 5, we present the simulation details and results of the polarizable model of acetonitrile. Our conclusions are briefly summarized in section 6.

2. Nonpolarizable Model and Simulation Details

We have employed the nonpolarizable model to carry out molecular dynamics simulations of the liquid−vapor interface of pure acetonitrile at two different temperatures: 298 and 273 K. The acetonitrile molecules are modeled as rigid objects with three interaction sites for short-range Lennard-Jones and long-range Coulomb interactions.[43] The methyl group is considered as a united atom with a single interaction site. In this models, the interaction between atomic sites of two different acetonitrile molecules is expressed as

$$u_{\alpha\beta}(r_\alpha, r_\beta) = 4\epsilon_{\alpha\beta}\left[\left(\frac{\sigma_{\alpha\beta}}{r_{\alpha\beta}}\right)^{12} - \left(\frac{\sigma_{\alpha\beta}}{r_{\alpha\beta}}\right)^{6}\right] + \frac{q_\alpha q_\beta}{r_{\alpha\beta}} \qquad (1)$$

where $r_{\alpha\beta}$ is the distance between the atomic sites α and β and q_α is the permanent partial charge of the $\alpha$the atom. The Lennard-Jones parameters $\sigma_{\alpha\beta}$ and $\epsilon_{\alpha\beta}$ are obtained by using the combination rules $\sigma_{\alpha\beta} = (\sigma_\alpha + \sigma_\beta)/2$ and $\epsilon_{\alpha\beta} = \sqrt{\epsilon_\alpha \epsilon_\beta}$. The values of the potential parameters q_α, σ_α, and ϵ_α for methyl, carbon and nitrogen sites are summarized in Table 1. These potential parameters give a dipole moment of 4.12 D for acetonitrile molecule and the experimental value is 3.92 D in the gas phase.[44] Although the dipole moment of acetonitrile in liquid phase is not known experimentally, it is expected to be somewhat higher than the corresponding gas-phase value. We also note that the above three-site model has been used earlier for studying pure acetonitrile and acetonitrile−water mixtures[31,43] and has been found to provide a reasonably good description of the behavior of acetonitrile in these systems.

TABLE 1: Values of the Lennard-Jones and Electrostatic Interaction Potential Parameters of Acetonitrile[a]

atom/ion	σ (Å)	ϵ (kJ/mol)	charge (e)
CH_3	3.60	1.589	+0.269
C	3.40	0.414	+0.129
N	3.30	0.414	−0.398

[a] e represents the magnitude of electronic charge.

TABLE 2: Values of the Diffusion Coefficients and Dipole Orientational Relaxation Times of Acetonitrile Molecules in Bulk Liquid and at Interfaces at 273 K and 298 K[a]

temp, K	N	D(bulk)	D_x(interface)	D_z(interface)	τ_μ(bulk)	τ_μ(interface)
273	864	2.30	8.10	2.35	7.25	3.7
298	864	3.0	9.75	3.54	4.65	2.45
298	1372	3.05	9.48	3.42	4.92	2.55

[a] The diffusion coefficients and the relaxation times are expressed in units of 10^{-5} cm^2 s^{-1} and ps, respectively.

We first carried out a bulk simulation in a cubic box of 864 acetonitrile molecules at 273 K and 864 or 1372 molecules at 298 K, periodically replicated in all three dimensions. The box length L was adjusted according to the experimental density of the bulk liquid at 298 and 273 K. After this bulk solution was properly equilibrated, two empty boxes of equal size were added on either side of the original simulation box along the z-dimension and this larger rectangular box (of dimension $L \times L \times 3L$) was taken as the simulation box in the next phase of the simulation run and the system was reequilibrated by imposing periodic boundary conditions in all three dimensions. This resulted in a liquid slab of approximate width L separated by vacuum layers of approximate width $2L$. Some of the acetonitrile molecules were found to vaporize to the empty space to form a liquid−vapor interface on both sides of the liquid slab. In Table 2, we have included the lengths of the simulation box along x and z dimensions at both temperatures. In the simulations, the long-range electrostatic interactions were treated by using the three-dimensional Ewald method.[45] The real space part of the Ewald summation was calculated by using the minimum image convention and the short-range Lennard-Jones interactions were calculated by using a spherical cutoff at distance $L/2$. We employed the quaternion formulation of the equations of rotational motion and, for the integration over time, we adapted the leapfrog algorithm with a time step of 10^{-15} s (1 fs). MD runs of 400 ps were used to equilibrate each system in the bulk phase and then the liquid−vapor interfacial systems in rectangular boxes were equilibrated for 500 ps. During the equilibration, the temperature of the simulation system was kept at 298 K or 273 K through rescaling of the velocities. The simulations of the interfacial systems were then continued in microcanonical ensemble for another 1000 ps (500 ps) for systems with 864 (1372) molecules. For all the systems, the total energy was found to be well conserved during the production phase of the simulations. Because the sizes of the present simulation systems are rather large, no significant effects of the Lennard-Jones potential cutoff at $L/2$ on the conservation of total energy were found. The average temperatures during

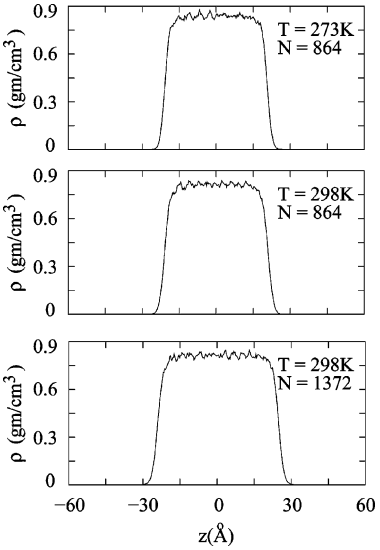

Figure 1. Dnesity profiles of acetonitrile molecules in the bulk and interfacial regions at 273 and 298 K

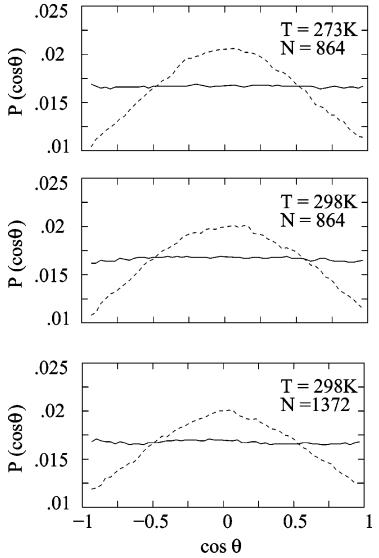

Figure 2. Probaility functions of the orientation of the dipole vector of acetonitrile molecules in the interfacial (dahsed) and bulk (solid) regions. θ denotes the angle between the dipole vector of an acetonitrile molecule and the surface normal.

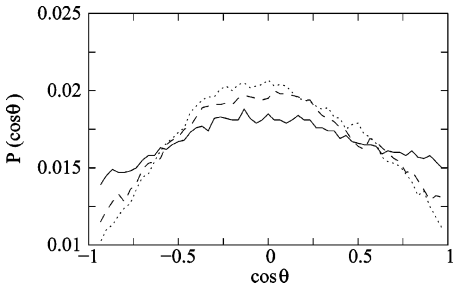

Figure 3. Dipolar orientational profile of acetonitrile molecules at the inner (solid), middle (dahsed), and outer (dotted) layer of the interface.

the production phase of the simulations were found to be 302 K (301 K) and 275 K for systems with 864 (1372) particles, and no systematic drift in the temperature of the simulation systems was observed. Since these average temperatures are very close the desired temperatures of 298 and 273 K, we will continue to use the latter values in subsequent discussions. The interfaces were found to be stable over the simulation time at both temperatures. The density and orientational profiles, surface tension, and the dynamical properties of the interfaces were calculated during the last production phase of the simulations, and the results are presented in the next section.

3. Results of the Nonpolarizable Model

3.1. Interfacial Structure and Surface Tension. We calculated the density profile of acetonitrile as a function of z by computing the average number of acetonitrile molecules in slabs of thickness $\Delta z = 0.05$ Å lying on either side of the central plane at $z = 0$, and the results are shown in Figure 1 at both the temperatures and for both system sizes at 298 K. Following previous work,[23,25,30] we define the thickness of a liquid−vapor interface as the distance over which the number density decreases from 90% to 10% of the bulk liquid density. The thickness obtained from the present simulations is 4.45 and 4.70 Å at 273 and 298 K, respectively, for $N = 864$ (N denotes the number of molecules) and 4.65 Å for $N = 1372$. We note that these values of the interfacial width include contributions from both the intrinsic width and the broadening due to capillary wave fluctuations as allowed by the length and time scales of the present simulations.[46−49] The decrease of temperature leads to a decrease of the interfacial width, which can be attributed to the presence of more number of acetonitrile molecules in the liquid region that exert attractive forces on the interfacial acetonitrile molecules and is consistent with a higher value of the surface tension at the lower temperature which is discussed in the later part of this section. Also, the effects of system size on the surface tension is found to be very small for the two systems investigated here at 298 K. We note that because there are very few molecules in the vapor phase of the simulation systems, accurate calculations of the vapor pressures of the systems could not be done in the present simulations.

In Figure 2, we have shown the orientational profiles of interfacial and bulk acetonitrile molecules. The interfacial region is defined by the 90−10 rule as described above and the rest of the region on the liquid side is taken as the bulk region. The average bulk density is found to be 0.80 and 0.82 g/cm^3 at 298 K and 273 K, which agree well with the experimental value of 0.79 g/cm^3 at 293 K.[44] The orientation of an acetonitrile molecule is described in terms of the angle θ that the molecular dipole vector makes with the surface normal along z-axis. In Figure 2, we have shown the results of the normalized probability function $P(\cos\theta)$ as a function of $\cos\theta$. In the bulk phase, the probability function is found to be uniform at both temperatures. Clearly, there is no preferred orientation of the acetonitrile molecules in the bulk phase of the liquid slabs as one would expect. In the interfacial region, however, the probability function is nonuniform, which shows an orientational structure of the interfacial molecules. At both temperatures, $P(\cos\theta)$ is maximum at $\cos\theta = 0$, which means that acetonitrile molecules at the interface prefer to orient with their dipoles parallel to the surface. This preferred parallel orientation of interfacial acetonitrile molecules is consistent with the recent experimental results based on second harmonic generation technique.[15] The slightly higher value of the maximum and a somewhat narrower distribution of the probability function around $\cos\theta = 0$ at the lower temperature show a higher degree of orientational ordering of the interfacial molecules with decrease of temperature. Again, the two systems of different sizes at 298 K are found to give essentially identical results for the orientational profiles. In Figure 3, we have further resolved the orientational structure of interfacial molecules by calculating the orientational profiles of three equally divided regions of the

interface: Inner, middle and the outer layers. The results of this figure are for $N = 864$ and $T = 298$ K. Clearly, the molecules at the outer interfacial layer are found to be orientationally more ordered than those of the inner layer at the interface which is more bulklike.

We calculated the surface tension by using the following virial expression, which is obtained from the well-known Kirkwood−Buff theory[50]

$$\gamma = \frac{1}{2A}\left\langle\left[\sum_{i<j}\sum_{\alpha,\beta}\frac{\partial u_{\alpha\beta}}{\partial r_{\alpha\beta}}\frac{1}{r_{\alpha\beta}}(\boldsymbol{r}_{ij}\cdot\boldsymbol{r}_{\alpha\beta} - 3z_{ij}z_{\alpha\beta})\right]\right\rangle \qquad (2)$$

where $u_{\alpha\beta}$ is the interaction energy between sites α and β on molecules i and j, r_{ij} and z_{ij} are the centers of mass distance and the distance along z direction between molecules i and j, and $r_{\alpha\beta}$ and $z_{\alpha\beta}$ are the corresponding distances between sites α and β. A is the total surface area which is equal to $2L^2$. We calculated the quantity within the third brackets in the above expression at each MD step, and finally the averaging was done over the total number of MD steps that were run during the production phase of the simulations. The average values of the calculated surface tension are found to be 40.7 and 42.8 at 298 and 273 K, respectively, for $N = 864$ and 41.0 at 298 K for $N = 1372$. The standard deviations of the surface tension data, which were calculated by using block averages over 100 ps, are about 7.5% of the average values reported above. At both temperatures, our calculated values of the surface tension are somewhat higher than the experimental values. For example, the experimental value of γ at 298 K is 26.3 as reported in ref 51. In ref 52, values of 29.10 and 27.80 are reported for the surface tension at 293 and 303 K, respectively. The discrepancy between the experimental and present simulation results may be due to the model of acetonitrile that we have employed in this work. The surface tension is known to be rather sensitive to the potential models and so the modeling of the methyl group as a united atom may be an important factor that contributes to this discrepancy.

3.2. Dynamics of Interfacial Molecules. In this section, we report the various dynamical properties of acetonitrile molecules at the liquid−vapor interface that we have calculated in the present work. An important issue concerning the dynamics of an interface is: How different is the dynamics of the interface compared to that of the corresponding bulk phases? The dynamical behavior of interfacial molecules is expected to be different from bulk molecules both translationally and rotationally. Also, the translational motion of acetonitrile molecules at the interface can be highly anisotropic in contrast to the bulk molecules, which move in an isotropic environment. In view of these points, we have separately calculated the perpendicular and parallel components of the translational diffusion and also the dipole orientational relaxation of both the interfacial and bulk molecules.

We denote the αth component of velocity of an acetonitrile molecule by $v_\alpha(t)$ ($\alpha = x, y, z$) and its normalized autocorrelation function $C_{v;\alpha}(t)$ is defined by

$$C_{v;\alpha}(t) = \frac{\langle v_\alpha(t)\, v_\alpha(0)\rangle}{\langle v_\alpha^{\,2}\rangle} \qquad (3)$$

where $\langle\cdots\rangle$ denotes an equilibrium ensemble average. The anisotropic nature of the translational motion is clearly illustrated in Figure 4 where we have shown the decay of the parallel (x) and perpendicular (z) components of the velocity−velocity autocorrelation function of interfacial acetonitrile molecules. In these calculations, the average of eq 3 is carried out over those molecules found in the interfacial region at time 0 and also at time t. The domain of the interfacial region is determined by the 90%−10% rule as described in the previous section. The results of the velocity relaxation of bulk acetonitrile molecules are also shown in this figure.

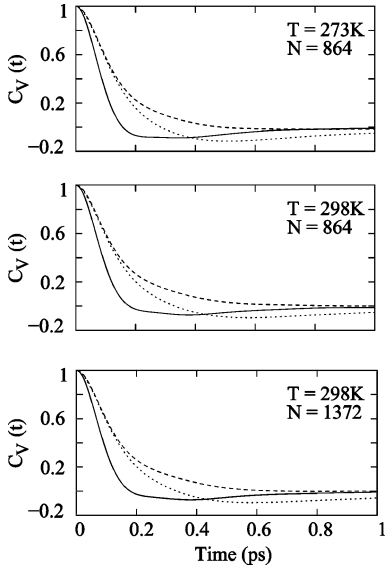

Figure 4. Time dependence of the x (dashed) and z (dotted) components of the velocity autocorrelation function of acetonitrile molecules in the interfacial region at 273 and 298 K. The solid curves show the results for acetonitrile molecules in the bulk liquid phase where the relaxation is isotropic.

The initial decay of both the parallel and the perpendicular components of the velocity autocorrelation function of interfacial molecules is found to be slower than that of the bulk acetonitrile molecules in the liquid phase. This slower velocity relaxation of interfacial molecules manifests a reduced collisional effect at the interfaces due to their lower density than that of the bulk liquid. The somewhat stronger negative values of the perpendicular velocity correlation function in the interfacial region at intermediate times show most likely the effects of dragging due to higher density in the liquid side and rebounce of molecules from the surface in the perpendicular direction. We have also calculated the diffusion coefficient D_α ($\alpha = x, y, z$) from the velocity−velocity autocorrelation function by using the following relation

$$D_\alpha = \frac{k_B T}{m}\int_0^\infty C_{v;\alpha}(t)\, dt \qquad (4)$$

where m is the mass of an acetonitrile molecule and k_B is the Boltzmann constant. The values of D_x and D_z of interfacial molecules are included in Table 2. We note that for interfacial molecules $D_x = D_y$. In this table we have also included the diffusion coefficients of bulk acetonitrile molecules for which the diffusion is isotropic. At room temperature, the bulk diffusion coefficient is found to be 3.05×10^{-5} cm^2 s^{-1} and the corresponding experimental value is 4.3×10^{-5} cm^2 s^{-1}.[53] The faster diffusion in the interfacial region is related to the slower relaxation of the corresponding velocity correlation that occurred due to the reduced density. In the perpendicular direction, the density of the liquid is much higher in the liquid side of the interface, which drags the interfacial molecules toward the liquid side. This dragging and the subsequent rebounce of acetonitrile molecules from the surfaces, which is present in the perpendicular motion but not in the parallel

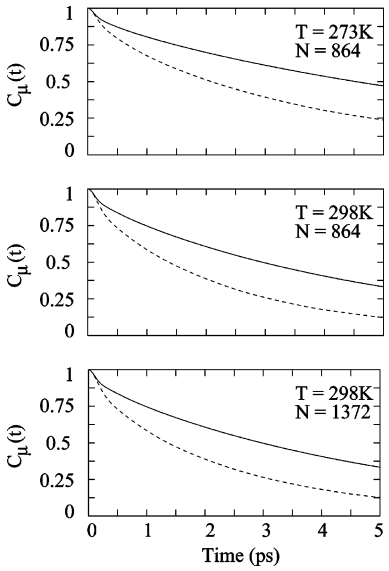

Figure 5. Relaxation of the self-dipole-correlation function of acetonitrile molecules at the interface (dashed) and in the bulk liquid phase (solid) at 273 and 298 K.

motion, is believed to be a primary reason for the slower net diffusion in the perpendicular direction than that in the parallel direction at the interfaces. We note that similar anisotropic diffusion of interfacial molecules has also been observed for liquid−vapor interfaces of water and aqueous solutions[27,30,54] and also of simple model dipolar systems such as Stockmayer fluids.[55]

The rotational motion of acetonitrile molecules at liquid−vapor interfaces is investigated by calculating the time dependence of the self-dipole-correlation function

$$C_\mu(t) = \frac{\langle \mu(t)\cdot\mu(0)\rangle}{\langle \mu(0)^2\rangle} \tag{5}$$

where $\mu(t)$ is the dipole vector of an acetonitrile molecule at time t. The results of $C_\mu(t)$ are shown in Figure 5 for both interfacial and bulk molecules at both the temperatures and also for both system sizes at 298 K. It is seen that the orientational relaxation at the interface occurs at a faster rate than that in the bulk. We define the orientational relaxation time τ_μ as the time integral of the orientational correlation function

$$\tau_\mu = \int_0^\infty C_\mu(t)\, \mathrm{d}t \tag{6}$$

where we have calculated the integral explicitly up to 4 ps by using the simulation data of $C_\mu(t)$ and the contribution of the tail part is obtained by using the fitted exponential functions. The results of the orientational relaxation times are also included in Table 2. The orientational relaxation time of interfacial acetonitrile molecules is found to be shorter than that of bulk molecules for both the temperatures considered here. We note that the density of acetonitrile molecules is low in the interfacial region and also interfacial molecules essentially do not have any solvation shell on the vapor side of the interface. Because of these reduced density and incomplete solvation effects, an acetonitrile molecule in the interfacial region experiences less rotational friction than that in the bulk phase. However, there is also an effect of orientational ordering for the interfacial molecules. We have shown in Figure 2 that the acetonitrile molecules at the interface prefer to orient parallel to the surface and this orientational structure imposes a constraint on the rotational motion of interfacial acetonitrile molecules. Clearly, the effects of reduced density appears to play a more important role in the rotational dynamics and we observe an enhanced rate of orientational relaxation of interfacial acetonitrile molecules. We note that similar faster relaxation of the interfacial molecules than the bulk ones have also been observed for liquid−vapor interfaces of other dipolar liquids and solutions.[30,54,55] The relative acceleration of the interfacial dynamics is, however, found to be somewhat higher for the acetonitrile interface than the corresponding aqueous interfaces. We also note that very similar dynamical results are found for both translational and rotational motion of acetonitrile molecules for two different system sizes that are considered here at 298 K. The dynamical results presented above at $T = 298$ K are averages over simulation trajectories of 1000 ps for $N = 864$ and 500 ps for $N = 1372$. To verify the convergence of the above results with respect to the length of simulation runs, we have also calculated the averages over the simulation trajectories of first 600 ps of the production run for $N = 864$, and the results are found to be very close to each other. For example, the values of D(bulk), D_x(interface), and D_z(interface) are found to be 3.05, 9.30, and 3.43, respectively, when averaged over 600 ps and are very close to the corresponding results of Table 2, which are averaged over 1000 ps. Thus, the results presented here can be considered as essentially converged with respect to the length of the simulation runs.

We also note that the difference between the interfacial and bulk dynamics of acetonitrile molecules is found to be slightly greater at 273 K than that at 298 K. For example, the ratios D_x(interface)/D(bulk) and τ(bulk)/τ(interface) are 3.25 and 1.9, respectively, at 298 K whereas these ratios become about 3.5 and 2.0, respectively, at 273 K. This increasing difference is caused by an increase of bulk liquid density that is in equilibrium with the interface. This increased density of the liquid slows down both translational and rotational motion of the bulk phase more than that at the interface and thus increases the relative difference between the time scales of interfacial and bulk dynamics.

4. Polarizable Model: Simulation Details and Results

The polarizable model of acetonitrile that we have employed in the current work is based on the charge-on-spring approach introduced earlier for modeling of water.[56,57] We note, however, that other methods are also available in the literature for inclusion of many-body polarization effects in molecular simulations such as the fluctuating charge model,[58−60] the model of dipoles on atomic sites,[61] and the self-consistent reaction field method.[62] In the current approach, the acetonitrile molecule has the same rigid geometry and Lennard-Jones interaction parameters as in the nonpolarizable model described in section 2. The permanent dipole moment is represented by fixed partial charges in methyl, carbon, and nitrogen atoms, and the induced dipole moment is represented by a pair of separated charges of fixed magnitude. Their distance determines the induced dipole moment. In the present model, one of the two charges (q_{pol}) resides on the carbon atom located at r, and the polarization charge ($-q_{\mathrm{pol}}$) is located at r' which is determined by the following equation

$$r' = r + \frac{\alpha}{q_{\mathrm{pol}}}\mathbf{E} \tag{7}$$

where α is the molecular polarizability. $\mathbf{E}$ is the electric field equal to $\mathbf{E}_0 + \mathbf{E}_{\mathrm{p}}$, where the first term is the field due to the

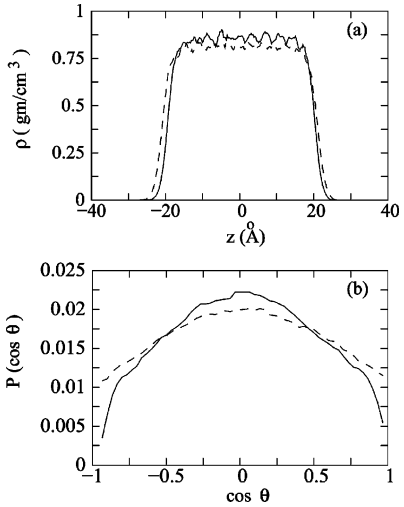

Figure 6. (a) Density and (b) orientational profiles of acetonitrile molecules for both polarizable (solid) and nonpolarizable (dashed) models at 298 K.

permanent charges and the second one corresponds to the field due to polarization charges. In the present work, we have used $q_{pol} = 8.0$ e and $\alpha = 4.48$ Å^3, where e is the magnitude of electronic charge. Variation of the polarization charge to 4.0 e or 12 e does not seem to alter the results presented here. As noted earlier in refs 56−57 and 63, because the contribution from the permanent charges will dominate the total electric field, the average effect of polarization due to other induced dipoles can be combined with the polarization from the permanent charges to save computational cost. Thus, we have employed a noniterative scheme where the first-order polarization effects are considered explicitly and the effects of field due to induced dipoles are taken into account implicitly by using a permanent dipole moment, which is slightly higher than the experimental dipole moment of an isolated acetonitrile molecule. We note that an earlier calculation of polarizable acetonitrile also employed a noniterative scheme.[63] A fully iterative scheme that goes beyond the first-order polarization effects will be considered in a future study. In the present noniterative polarizable model, we have used the following permanent charges on different sites of the acetonitrile molecule: $q_{CH_3} = 0.26093$ e, $q_C = 0.12513$ e (excluding q_{pol}), and $q_N = -0.38606$ e. The above partial charges produce a permanent dipole moment of 4 D, and the experimental value is 3.92 D. The slightly higher value of the permanent dipole moment of the polarizable model as compared to the experimental value takes into account the higher order polarization effects in an effective manner as discussed above.

The simulation system of the polarizable acetonitrile consisted of 864 molecules at 298 K. The simulation method was similar to the one described earlier for the nonpolarizable model. The system was equilibrated for 200 ps in the bulk phase and then, as before, two empty boxes were added on either side of the original box along the *z*-direction and the resultant interfacial system was equilibrated for 400 ps. Finally, the production run was continued for another 400 ps, over which the various equilibrium and dynamical properties were calculated.

In Figure 6, we have shown the results of density and orientation profiles of acetonitrile molecules for the polarizable model. The results of nonpolarizable model are also included in this figure for comparison. For both density and orientational profiles, the results of the polarizable model are found to be qualitatively similar to those of the nonpolarizable model. At the quantitative level, the thickness of the liquid slab is found to be slightly smaller, hence a slightly higher bulk liquid density, for the polarizable model. Also, the orientational distribution of the interfacial molecules is found to be somewhat narrower for the polarizable model as compared to that for the nonpolarizable model. Both these results reveal a somewhat stronger cohesion between the acetonitrile molecules for the polarizable model. This observation is consistent with the somewhat slower dynamics of polarizable acetonitrile molecules, as shown by the smaller values of diffusion coefficients and higher values of orientational relaxation times that are included in Table 3. In Figure 7, we have shown the variation of the dipole moment of acetonitrile molecules across the liquid−vapor interfaces. It is seen that, as we move from the liquid phase to the vapor phase, the dipole moment changes from 4.65 to 4.0 D, which is the gas-phase dipole moment value for the present model.

TABLE 3: Values of the Diffusion Coefficients and Dipole Orientational Relaxation Times of Polarizable Acetonitrile Molecules in Bulk Liquid and at Interfaces at 298 K[a]

D (bulk)	D_x(interface)	D_z(interface)	τ_μ(bulk)	τ_μ(interface)
1.75	7.5	1.8	10.75	5.75

[a] The diffusion coefficients and the relaxation times are expressed in units of 10^{-5} cm^2 s^{-1} and ps, respectively.

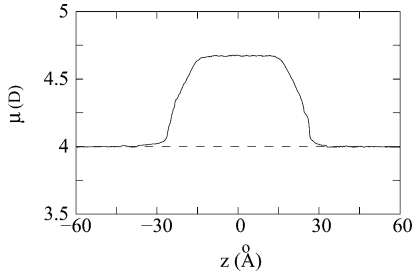

Figure 7. Change of dipole moment of acetonitrile molecules across the liquid−vapor interface. The dahsed line corresponds to the gas phase dipole moment of an acetonitrile molecule as given by the present polarizable model.

5. Conclusion

We have performed molecular dynamics simulations to investigate the various equilibrium and dynamical properties of acetonitrile liquid−vapor interface. Simulations are carried out at room temperature and also at a lower temperature and both nonpolarizable and polarizable models are considered. Various interfacial properties such as the inhomogeneous density and orientational profiles, the width of the interface, surface tension, molecular diffusion, and orientational relaxation are calculated in the present study.

It is found that the dipole vectors of the interfacial acetonitrile molecules tend to orient parallel to the surface. The degree of orientational order at the interface is found to be more at the lower temperature. The width of the interface, which is calculated by using the 90%−10% rule, is found to decrease and the surface tension is found to increase with decrease of temperature. Overall, the acetonitrile liquid−vapor interface is characterized by a larger width and smaller surface tension when compared to an aqueous liquid−vapor interface.[30]

The translational motion of acetonitrile molecules is found to be highly anisotropic in the interfacial region. The relaxation of the velocity autocorrelation function shows a reduced cage effect for interfacial molecules. The diffusion along the parallel direction is found to be about 3 times faster than that in the perpendicular direction at the interface. Even the perpendicular diffusion at the interface is somewhat faster than that in the

bulk phase, which is attributed to the effects of reduced density in the interfacial region. The orientational motion of acetonitrile molecules at the interface is also found to be about 2 times faster than that of bulk molecules. The difference between the interfacial and bulk dynamics is found to be slightly larger at 273 K than that at 298 K, which is attributed to a slightly higher density of the liquid phase at the lower temperature.

Also, at 298 K, the simulations are carried out for two different system sizes using the nonpolarizable model: One with 864 molecules and the other with 1372 molecules. Very similar results are found for these two systems, and thus the convergence of the results with respect to the size of the simulation systems is ensured. The results presented here are also shown to be essentially converged with respect to the length of the simulation runs that are considered in this work.

Finally, we also employed a polarizable model of acetonitrile to study the behavior of its liquid−vapor interface at 298 K. The results of the polarizable model are found to be qualitatively similar to those of the nonpolarizable model. However, at the quantitative level, the polarizable model shows enhanced cohesion between the acetonitrile molecules, leading to a slightly smaller interfacial width, narrower orientational distribution of interfacial molecules, and a slower dynamics than those of the nonpolarizable model. Also, the polarizable model shows that the dipole moment of acetonitrile molecules changes rather sharply across the interface from 4.65 D to its gas phase value of 4.0 D. We note that such variation of the dipole moment across the interface could not be obtained by using the nonpolarizable model. We also note that the present polarizable model is based on a noniterative scheme that includes the polarization effects explicitly up to first order. It would be interesting to develop a fully iterative scheme within the present charge-on-spring model where the higher order polarization effects are included explicitly. Such a model is expected to give better results for the structure and dynamics of both bulk and interfacial regions. Work in this direction is in progress.

Acknowledgment. We gratefully acknowledge the financial support from the Council of Scientific and Industrial Research (CSIR) and Department of Science and Technology (DST), Government of India.

References and Notes

(1) Eisenthal, K. B. *Chem. Rev.* **1996**, *96*, 1343 and references therein.
(2) Benjamin, I. *Chem. Rev.* **1996**, *96*, 1449 and references therein.
(3) Du, Q.; Freysz, E.; Shen, Y. R. *Science* **1994**, *264*, 826. Du, Q.; Superfine, R.; Freysz, E.; Shen, Y. R. *Phys. Rev. Lett.* **1993**, *70*, 2313.
(4) Goh, M. C.; Hicks, J. M.; Kemnitz, K.; Pinto, G. R.; Bhattacharyya, K.; Eisenthal, K. B.; Heinz, T. F. *J. Phys. Chem.* **1988**, *92*, 5074.
(5) Sitzmann, E. V.; Eisenthal, K. B. *J. Phys. Chem.* **1988**, *92*, 4579.
(6) Kemnitz, K.; Bhattacharyya, K.; Hicks, J. M.; Pinto, G. R.; Eisenthal, K. B.; Heinz, T. F. *Chem. Phys. Lett.* **1986**, *131*, 285.
(7) Bhattacharyya, K.; Sitzmann, E. V.; Eisenthal, K. B. *J. Chem. Phys.* **1987**, *87*, 1442.
(8) Petralli-Mallow, T.; Wong, T. M.; Byers, J. D.; Yee, H. I.; Hicks, J. M. *J. Phys. Chem.* **1993**, *97*, 1383.
(9) Superfine, R.; Huang, J. Y.; Shen, Y. R. *Opt. Lett.* **1990**, *15*, 1276.
(10) Conboy, J. C.; Daschbach, J. L.; Richmond, G. L. *J. Phys. Chem.* **1994**, *98*, 9688.
(11) Raising, T.; Stehlin, T.; Shen, Y. R.; Kim, M. W.; Valint, P., Jr. *J. Chem. Phys.* **1988**, *89*, 3386.
(12) Shi, X.; Borguet, E.; Tarnovski, A. N.; Eisenthal, K. B. *Chem. Phys.* **1996**, *205*, 167.
(13) Zimdars, D.; Eisenthal, K. B. *J. Phys. Chem. B* **2001**, *105*, 3993.
(14) Zhang, D.; Gutow, J. H.; Eisenthal, K. B.; Heinz, T. F. *J. Chem. Phys.* **1993**, *98*, 5099.
(15) Kim, J.; Chou, K. C.; Somorjai, G. A. *J. Phys. Chem. B* **2003**, *107*, 1592.
(16) Hayter, J. B.; Penfold, J. *J. Chem. Soc., Faraday Trans.* **1981**, *77*, 1851.
(17) Chen, S.-H. *Annu. Rev. Phys. Chem.* **1986**, *37*, 351.
(18) *Physicochemical Hydrodynamics*; Velarde, M. G., Ed.; Plenum: New York, 1988.
(19) Raina, G.; Kulkarni, G. U.; Rao, C. N. R. *J. Phys. Chem. A* **2001**, *105*, 10204.
(20) Pohorille, A.; Benjamin, I. *J. Chem. Phys.* **1991**, *94*, 5599.
(21) Matsumoto, M.; Takaoka, Y.; Kataoka, Y. *J. Chem. Phys.* **1993**, *98*, 1464.
(22) Eggebrecht, J.; Thompson, S. M.; Gubbins, K. E. *J. Chem. Phys.* **1987**, *86*, 2299.
(23) Taylor, R. S.; Dang, L. X.; Garrett, B. C. *J. Phys. Chem.* **1996**, *100*, 11720.
(24) Sokhan, V. P.; Tildesley, D. J. *Mol. Phys.* **1997**, *92*, 625.
(25) Alejandre, J.; Tildesley, D. J.; Chapela, G. A. *J. Chem. Phys.* **1995**, *102*, 4574.
(26) Yeh, Y. L.; Zhang, C.; Held, H.; Mebel, A. M.; Wei, X.; Lin, S. H.; Shen, Y. R. *J. Chem. Phys.* **2001**, *114*, 1837.
(27) Stuart, S. J.; Berne, B. J. *J. Phys. Chem. A* **1999**, *103*, 10300. Liu, P.; Harder, E.; Berne, B. J. *J. Phys. Chem. B* **2004**, *108*, 6595.
(28) Jungwirth, P.; Tobias, D. J. *J. Phys. Chem. B* **2000**, *104*, 7702; *J. Phys. Chem. B* **2001**, *105*, 10468; *J. Phys. Chem. B* **2002**, *106*, 6361.
(29) Senapati, S. *J. Chem. Phys.* **2002**, *117*, 1812.
(30) Paul, S.; Chandra, A. *Chem. Phys. Lett.* **2003**, *373*, 87.
(31) Mountain, R. D. *J. Phys. Chem. B* **2001**, *105*, 6556.
(32) Chang, T.-M.; Dang, L. X. *J. Phys. Chem. B* **2005**, *109*, 5759.
(33) Chanda, J.; Chakraborty, S.; Bandyopadhyay, S. *J. Phys. Chem. B* **2005**, *109*, 471. Bandyopadhyay, S.; Chanda, J. *Langmuir* **2003**, *19*, 10443.
(34) Paul, S.; Chandra, A. *J. Chem. Phys.*, in press.
(35) Matsumoto, M.; Mizukuchi, H.; Kataoka, Y. *J. Chem. Phys.* **1993**, *98*, 1473.
(36) Gubbins, K. E. *Chem. Phys. Lett.* **1980**, *76*, 329. Thompson, S. M.; Gubbins, K. E.; Haile, J. M. *J. Chem. Phys.* **1981**, *75*, 1325.
(37) Frodl, P.; Dietrich, S. *Phys. Rev. E* **1993**, *48*, 3741.
(38) Yang, B.; Sullivan, D. E.; Gray, C. G. *J. Phys.: Condens. Matter* **1994**, *6*, 4823.
(39) Hirata, Y. *J. Phys. Chem. A* **2002**, *106*, 2187.
(40) Takamuku, T.; Tabata, M.; Yamaguchi, A.; Nishimoto, J.; Kumamoto, M.; Wakita, H.; Yamaguchi, T. *J. Phys. Chem. B* **1998**, *102*, 8880.
(41) Mountain, R. D. *J. Phys. Chem. A* **1999**, *103*, 10744.
(42) Bergman, D. L.; Laaksonen, A. *Phys. Rev. E* **1998**, *58*, 4706.
(43) Edwards, D. M. F.; Maden, P. A.; McDonald, I. R. *Mol. Phys.* **1984**, *51*, 1141. Molinero, V.; Laria, D.; Kapral, R. *J. Chem. Phys.* **1998**, *109*, 6844.
(44) *CRC Handbook of Chemistry and Physics*; Weast, R. C., et al., Eds.; CRC Press: Boca Raton, FL, 1989.
(45) Allen, M. P.; Tildesley, D. J. *Computer Simulation of Liquids*; Clarendon Press: Oxford, 1987.
(46) Lacasse, M.-D.; Grest, G. S.; Levine, A. J. *Phys. Rev. Lett.* **1998**, *80*, 309.
(47) Sides, S. W.; Grest, G. S.; Lacasse, M.-D. *Phys. Rev. E* **1999**, *60*, 6708.
(48) Werner, A.; Schmid, F.; Müller, M.; Binder, K. *Phys. Rev. E* **1999**, *59*, 728.
(49) Senapati, S.; Berkowitz, M. L. *Phys. Rev. Lett.* **2001**, *87*, 176101.
(50) Kirkwood, J. G.; Buff, F. P. *J. Chem. Phys.* **1949**, *17*, 338.
(51) Teixeira, P. I. C.; Almeida, B. S.; Telo da Gama, M. M.; Rueda, J. A.; Rubio, R. G. *J. Phys. Chem.* **1996**, *96*, 8488.
(52) Timmermans, J. *Physico-Chemical Constants of Pure Organic Compounds*; Elsevier Publishing Company Inc.: Amsterdam, 1950.
(53) Hurle, R. L.; Woolf, L. A. *J. Chem. Soc., Faraday Trans. 1* **1982**, *78*, 2233.
(54) Paul, S.; Chandra, A. *J. Chem. Theo. Comput.*, in press; *J. Chem. Phys.*, in press.
(55) Paul, S.; Chandra, A. *J. Phys. Chem. B* **2003**, *107*, 12705.
(56) Straatsma, T. P.; McCammon, J. A. *Mol. Simul.* **1990**, *5*, 181.
(57) Yu, H.; Hansson, T.; van Gunsteren, W. F. *J. Chem. Phys.* **2003**, *118*, 221.
(58) Rick, S. W.; Stuart, S. J.; Berne, B. J. *J. Chem. Phys.* **1994**, *101*, 6141.
(59) Rick, S. W. *J. Chem. Phys.* **2001**, *114*, 2276.
(60) Patel, S.; Brooks, C. L., III. *J. Chem. Phys.* **2005**, *122*, 24508.
(61) Koneshan, S.; Rasaiah J. C.; Dang, L. X. *J. Chem. Phys.* **2001**, *114*, 7544.
(62) Luque, F. J.; Bofill, J. M.; Orozco, M. *J. Chem. Phys.* **1995**, *103*, 10183.
(63) Markovich, G.; Perera L.; Berkowitz M. L.; Cheshnovsky O. *J. Chem. Phys.* **1996**, *105*, 2675.